Robust Model Reduction for a Flexible Spacecraft

Ashish Tewari*
Indian Institute of Technology, Kanpur 208016, India

I. Introduction

THE problem of controlling flexible spacecraft in the presence of modeling uncertainties becomes challenging when reduced-order controllers are required to be implemented on an onboard computer with limited speed and memory. Among the several alternatives available for reducing the plant model size, the most systematic approaches are those employing an uncertainty model for the plant, wherein an H_∞ norm error bound guarantees the robustness of the reduced-order model in a specific frequency range, thereby allowing the design of a controller with a desired bandwidth. Such algorithms can be subdivided into those that represent the modeling error as additive or multiplicative uncertainty. This Note applies both additive and multiplicative error models to a flexible spacecraft example and compares their accuracy with an approximate finite element model (FEM) of the same size as the H_∞ norm bounded model. In this specific case, it is seen that the best robustness properties are exhibited by the reduced FEM.

II. Robust Model Reduction Techniques

Given the prescribed control-system bandwidth, it is possible to derive a reduced plant model using the modeling error represented by either an additive or a multiplicative unstructured uncertainty.

A. Additive Uncertainty Model

If $\boldsymbol{G}(s)$ is the transfer-function matrix of the full-order plant and $\boldsymbol{G}_{\boldsymbol{k}}(s)$ that of a kth-order reduced model, then the additive modeling error is defined as an additive uncertainty at the plant output given by

$$\Delta_A(s) = \boldsymbol{G}(s) - \boldsymbol{G}_k(s) \tag{1}$$

For such a model an upper bound for the achievable control bandwidth is provided by the additive robust frequency ω_{rA} defined as

$$\omega_{rA} = \max\{\omega \mid \sigma_{\min}[\boldsymbol{G}_k(j\omega)] \geq \sigma_{\max}[\Delta_A(j\omega)]\} \tag{2}$$

where $\sigma_{\min}$ and $\sigma_{\max}$ are the smallest and largest singular values. If Δ_A is stable, then Eq. (2) provides a sufficient (but not necessary) condition that the closed-loop plant will not be destabilized by the modeling error if the control bandwidth is less than ω_{rA}. There are several algorithms available to carry out additive uncertainty model reduction, and they can be broadly divided into balanced realization and Hankel approximation.

Balanced Realization

For a reduced-order state-space realization $(\boldsymbol{A}_k, \boldsymbol{B}_k, \boldsymbol{C}_k, \boldsymbol{D}_k)$ of an asymptotically stable system, the Lyapunov equations

$$\boldsymbol{A}_k\boldsymbol{P} + \boldsymbol{P}\boldsymbol{A}_k^T + \boldsymbol{B}_k\boldsymbol{B}_k^T = \boldsymbol{0} \tag{3a}$$

$$\boldsymbol{A}_k^T\boldsymbol{Q} + \boldsymbol{Q}\boldsymbol{A}_k + \boldsymbol{C}_k^T\boldsymbol{C}_k = \boldsymbol{0} \tag{3b}$$

must have a common solution $\boldsymbol{P} = \boldsymbol{Q} = \Sigma$, where $\boldsymbol{P}$ and $\boldsymbol{Q}$ are the controllability and observability gramians, respectively, and Σ is a diagonal matrix. By using a factorization, such as Cholesky decomposition, $\boldsymbol{Q} = \boldsymbol{R}^T\boldsymbol{R}$, and a singular value decomposition, $\boldsymbol{R}\boldsymbol{P}\boldsymbol{R}^T = \boldsymbol{U}\Sigma^2\boldsymbol{U}^T$, a balanced realization can be obtained as

$$(\boldsymbol{A}_k, \boldsymbol{B}_k, \boldsymbol{C}_k, \boldsymbol{D}_k) = (\boldsymbol{T}\boldsymbol{A}\boldsymbol{T}^{-1}, \boldsymbol{T}\boldsymbol{B}, \boldsymbol{C}\boldsymbol{T}^{-1}, \boldsymbol{D}) \tag{4}$$

where $\boldsymbol{T} = \Sigma^{-1/2}\boldsymbol{U}^T\boldsymbol{R}$. It can be shown[1] that the H_∞ norm associated with the kth-order reduced model with a minimal, balanced realization is given by

$$\|\boldsymbol{G}(s) - \boldsymbol{G}_k(s)\|_\infty \leq 2\sum_{i=k+1}^{N}\sigma_i \tag{5}$$

where N is the order of the original (full-order) plant and σ_i are the Hankel singular values obtained from $\Sigma = \text{diag}\{\sigma_i, \ldots, \sigma_N\}$. More robust balanced realization algorithms are the truncated square-root balancing (TBR)[2] and Schur balancing (SMR),[2] which avoid computing a minimal realization of $\boldsymbol{G}(s)$. They can also handle unstable systems by splitting $\boldsymbol{G}(s)$ into stable and antistable parts. However, the TBR algorithm can be ill conditioned for a strongly controllable and weakly observable (or vice versa) system.

Hankel Approximation

The Hankel approximation is based upon the theorem by Glover[3] that given a rational $\boldsymbol{G} \in \boldsymbol{H}_\infty$, then for any $\boldsymbol{Y} \in \boldsymbol{H}_\infty$,

$$\|\boldsymbol{G}\|_H \leq \|\boldsymbol{G} + \boldsymbol{Y}^*\|_\infty \tag{6}$$

where $\|\boldsymbol{G}\|_H = \sigma_{\max}[(\boldsymbol{P}\boldsymbol{Q})^{1/2}]$ is the Hankel norm of $\boldsymbol{G}$ and $\boldsymbol{Y}^*(s) = \boldsymbol{Y}^T(-s)$. The Hankel approximation problem is, thus, approached as minimization of $\|\boldsymbol{G} + \boldsymbol{Y}_{\text{opt}}^*\|_\infty$ with respect to $\boldsymbol{Y} \in \boldsymbol{H}_\infty$, such that the optimal solution $\boldsymbol{Y}_{\text{opt}}$ obeys

$$\left\|\boldsymbol{G} + \boldsymbol{Y}_{\text{opt}}^*\right\|_\infty = \|\boldsymbol{G}\|_H \tag{7}$$

Glover[3] devised an algorithm for this minimization problem, which required an initial balanced realization of $\boldsymbol{G}$. This ill-conditioned step is bypassed by algorithm of Sofonov et al. (OHR),[4] which solves the Lyapunov equations [Eqs. (3a) and (3b)] to find the gramians $\boldsymbol{P}$ and $\boldsymbol{Q}$ for any realization of $\boldsymbol{G}$.

B. Multiplicative Uncertainty Model

The relative error of approximating the plant $\boldsymbol{G}(s)$ with a reduced-order model $\boldsymbol{G}_k(s)$ can be represented by a multiplicative unstructured uncertainty Δ_M appearing at the plant output such that

$$\Delta_M = (\boldsymbol{G} - \boldsymbol{G}_k)^{-1} \tag{8}$$

Equation (8) yields the following sufficient condition for stability:

$$\sigma_{\max}(\Delta_M) < 1/\sigma_{\max}[\boldsymbol{G}\boldsymbol{K}(\boldsymbol{I} + \boldsymbol{G}\boldsymbol{K})^{-1}] \tag{9}$$

The multiplicative robust frequency ω_{rM} can then be defined as

$$\omega_{rM} = \max\{\omega \mid \sigma_{\max}(\Delta_M) \leq 1\} \tag{10}$$

This implies that the closed-loop stability can be ensured if the control bandwidth is less than ω_{rM}. It can be shown that

$$\sigma_{\max}(\Delta_M) \geq \frac{\sigma_{\max}(\Delta_A)}{\sigma_{\min}(\boldsymbol{G})} \tag{11}$$

which implies that $\omega_{rM} \geq \omega_{rA}$. A balanced stochastic truncation algorithm using the Schur method (SBST) minimizing the relative error given by

$$\left\|\boldsymbol{G}^{-1}(\boldsymbol{G} - \boldsymbol{G}_k)\right\|_\infty \leq \sum_{i=k+1}^{N}\frac{2\sigma_i}{1 - \sigma_i} \tag{12}$$

has been developed by Safonov and Chiang.[5] This method computes the controllability gramian $\boldsymbol{P}$ of $\boldsymbol{G}(s)$ and observability gramian $\boldsymbol{Q}$ of the minimum phase left spectral factor of $\boldsymbol{G}(s)\boldsymbol{G}^T(-s)$.

Received Oct. 2, 1997; revision received April 20, 1998; accepted for publication May 5, 1998.

*Assistant Professor, Department of Aerospace Engineering. Senior Member AIAA.

III. Numerical Results

Consider a rotating spacecraft[6] modeled as a rigid hub and four flexible appendages with tip masses. The appendages are modeled as Euler–Bernoulli beams, and an FEM approximation is used for small elastic displacements measured with respect to rotating hub-fixed axes. Radial deformations and nonlinear kinematics of beam elongation are neglected. The control inputs are three externally applied torques, acting on the hub, the end of appendages 1 and 2, and the end of appendages 3 and 4, respectively. Three sensors collocated with the actuators generate the hub rotation angle, end rotation of appendages 1 and 2, and end rotation of appendages 3 and 4, as the three outputs. Because the deformations are antisymmetric, the generalized displacement vectors for appendages 1 and 2 are the same, and those for appendages 3 and 4 are the same. The total order of the FEM model is $(8n + 2)$, where n is the number of finite elements in each appendage. A comparison of various model reduction techniques applied to the 162-order plant given by 20 finite elements/appendage is carried out in Fig. 1, which shows the largest singular-value plots of the 162-order plant and 26-order reduced-models by the TBR, SMR, OHR, and SBST methods. The SMR, OHR, and SBST models fail to accurately represent the first three modes and display incorrect frequencies and magnitudes of higher modes. The TBR model is seen to be the closest in comparison with the full-order plant, among the 26-order H_∞-norm-based methods. Figure 2 shows that a 26-order reduced FEM model (obtained with three elements/appendage) is in excellent agreement with the 162-order plant as far as the first eight modes are concerned (frequency below 60,000 rad/s), whereas a TBR model of the same order has comparatively very large errors. Although the singular value Bode plots are a measure of a reduced model's accuracy vis-à-vis the full-order plant, the critical test of a model is in the design of a controller. To assess the performance of controllers based on reduced plants, optimal controllers are designed by the linear quadratic Gaussian (LQG) method based on the 26-order reduced models. The

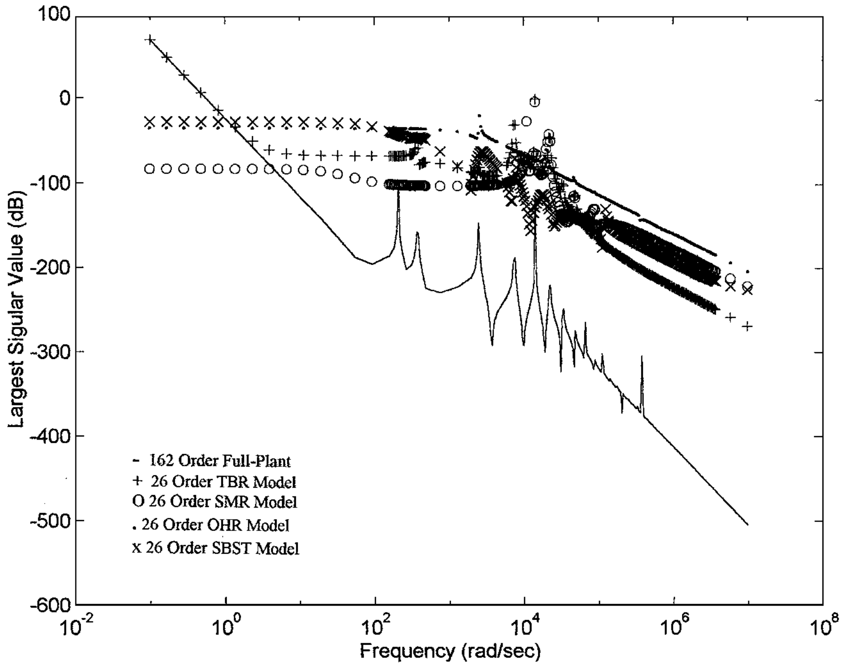

Fig. 1 Largest singular value of the H_∞ -based reduced-order models compared with the full-order plant.

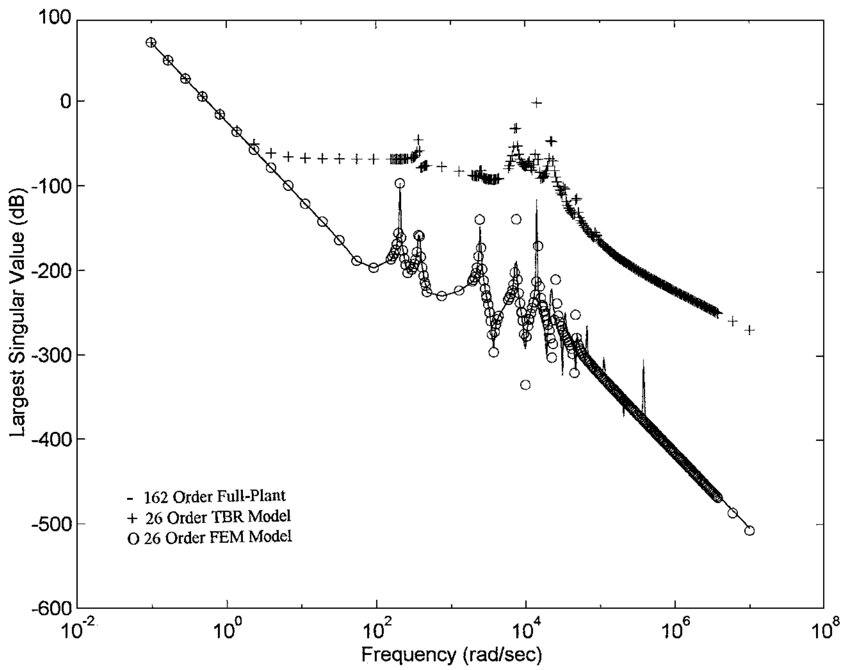

Fig. 2 Largest singular value of 26-order FEM and TBR models compared with the full-order plant.

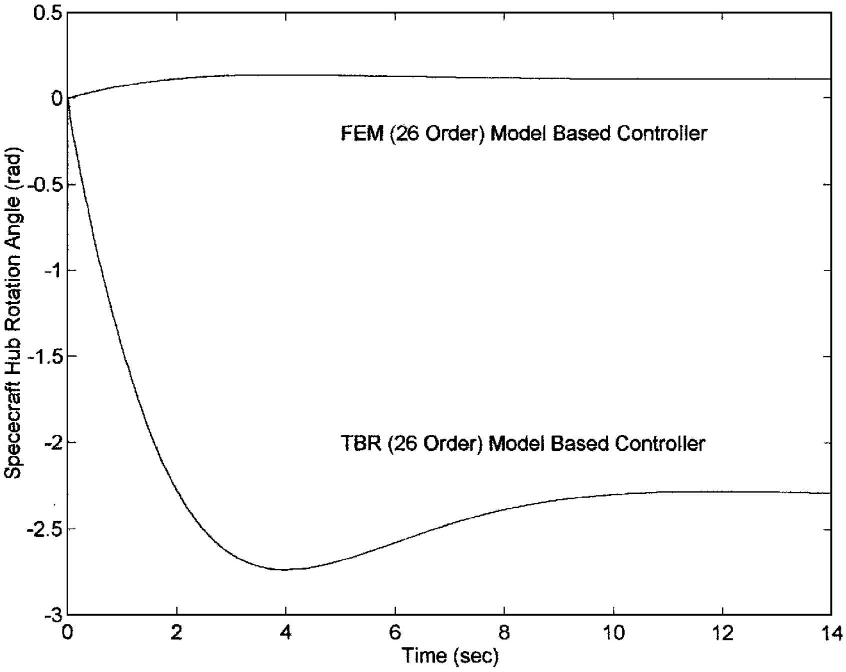

Fig. 3 Step response of the FEM and TBR reduced-model-based LQG closed-loop system.

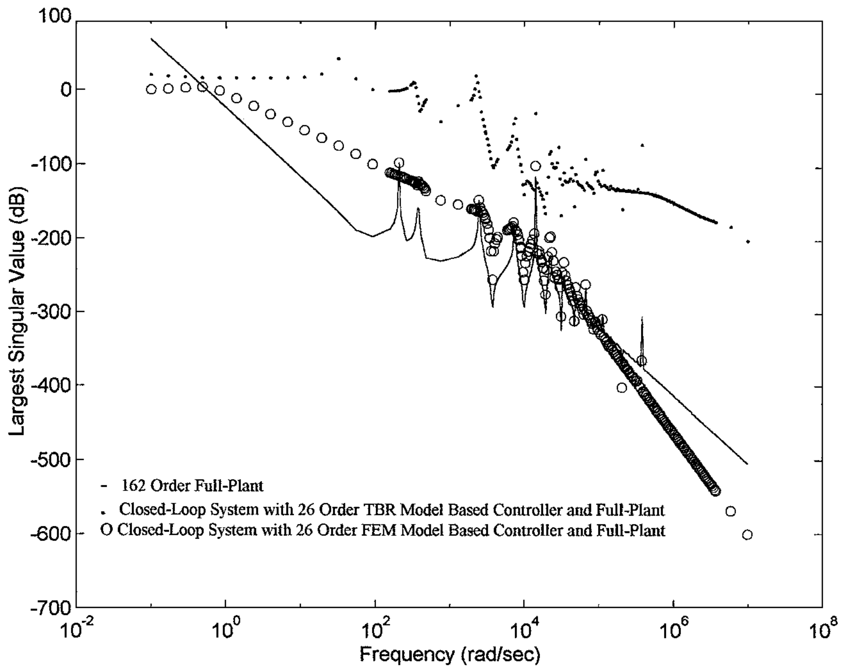

Fig. 4 Largest singular value of the FEM and TBR reduced LQG controllers applied to the full-order plant.

design criteria are to achieve a stabilization of the resonant modes with a bandwidth of 10^5 rad/s and a -20 dB/decade rolloff in each signal direction at high frequencies. Figure 3 shows the closed-loop response of FEM and TBR reduced-model compensators for a step demand on the spacecraft hub rotation angle. Although the controllers designed for both of the models stabilize the respective reduced-order model within the prescribed limits, their performance is seen to deteriorate when applied to the full-order plant (Fig. 4). The closed-loop behavior of the 26-order FEM controller is seen to be far superior to that of the TBR controller of the same order, when applied to the full-order plant.

IV. Conclusion

An assessment of various additive and multiplicative error model-reduction techniques based on H_∞ norm bound, applied to the stabilization of a symmetric flexible spacecraft example, shows that even though the robustness of such model-reduction algorithms is guaranteed within a prescribed bandwidth, they do not always lead to an optimal controller that can stabilize the full-order plant. In contrast, a reduced FEM of the same order yields controllers with much better robustness characteristics than any of the norm bounded reduction schemes.

References

[1]Moore, B. C., "Principal Component Analysis in Linear System: Controllability, Observability, and Model Reduction," *IEEE Transactions on Automatic Control*, Vol. AC-26, No. 1, 1981, pp. 17–31.

[2]Safonov, M. G., and Chiang, R. Y., "Schur Balanced Model Reduction," American Control Conf. (Atlanta, GA), June 1988.

[3]Glover, K., "All Optimal Hankel Norm Approximation of Linear Multivariable Systems, and Their L_∞ Error Bounds," *International Journal of Control*, Vol. 39, No. 6, 1984, pp. 1145–1193.

[4]Safonov, M. G., Chiang, R. Y., and Limebeer, D. J. N., "Hankel Model Reduction Without Balancing—A Descriptor Approach," *Proceedings of IEEE Conference on Decision and Control* (Los Angeles, CA), Inst. of Electrical and Electronics Engineers, New York, 1987.

[5]Safonov, M. G., and Chiang, R. Y., "Model Reduction for Robust Control: A Schur Relative-Error Method," American Control Conf. (Atlanta, GA), June 1988.

[6]Junkins, J. L., and Kim, Y., *Introduction to Dynamics and Control of Flexible Structures*, AIAA Education Series, AIAA, Washington, DC, 1993, pp. 206–211.

Effects of Gravitation on Time-Optimal Control of Two-Link Manipulators

Reza Fotouhi-Chahouki* and Walerian Szyszkowski†
University of Saskatchewan,
Saskatoon, Saskatchewan S7N 5A9, Canada

I. Introduction

EFFECTS of orientation of the plane of motion in the gravitational field of a two-link manipulator on the time and the control pattern of optimal maneuvers are examined. Time-optimal maneuvers are determined by solving directly the two-point boundary value problem (TPBVP) derived from Pontryagin's minimum principle. The solutions are generated by the numerical procedure, which is discussed in more detail in Refs. 1 and 2, that combines the forward-backward method with the shooting method.

In general, the TPBVPs are extremely difficult to solve numerically despite their elegant mathematical form. Computational difficulties with convergence are usually attributed to the costates. The numerical solutions to time-optimal control problems presented in the literature were obtained using mostly the parametrization technique,[3,4] in which the calculation of costates is not necessary. In Ref. 3 it was concluded that for two-link manipulators "the probability for a bang-bang solution with more than three switches to satisfy Pontryagin's minimum principle is almost zero." We found this conclusion, in general, not valid. For two-link manipulators we were able to obtain numerous time-optimal bang-bang control solutions with four switches directly by solving the TPBVP.[5] Also, here, it is shown that two optimal maneuvers with identical initial and final conditions will have either three or four switches depending on the orientation of the plane of motion.

II. Time-Optimal Control of Manipulators

Maneuvers of a two-link manipulator are considered in plane y, z oriented with respect to the vertical as shown in Fig. 1.

The effective gravitational acceleration depends on angle β and is equal to $g = g_0 \sin(\beta)$. The manipulator is driven by the motors installed at the shoulder and the elbow joints and generating the torques u_1 and u_2, respectively.

In terms of the states x where $x_1 = \varphi_1$, $x_2 = \dot{\varphi}_1$, $x_3 = \varphi_2$, and $x_4 = \dot{\varphi}_2$, the equation of motion of the manipulator can be obtained in the form[1,6]

$$\dot{x}(t) = A(x, g) + C(x)u(t) \tag{1}$$

where A and C are a vector and a matrix of nonlinear functions of states x and gravity g, and u is a vector of controls. The control torques are bounded as

$$U_i^- \le u_i(t) \le U_i^+ \tag{2}$$

Received Aug. 20, 1997; revision received Feb. 3, 1998; accepted for publication June 1, 1998.

*Research Associate, Mechanical Engineering Department, 57 Campus Drive.

†Professor, Mechanical Engineering Department, 57 Campus Drive.

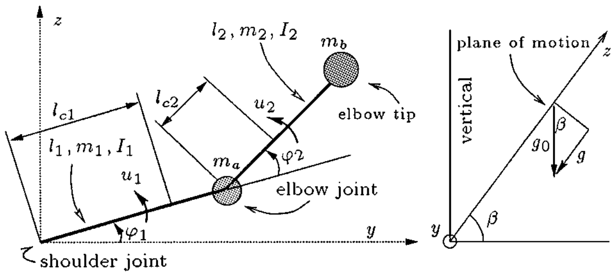

Fig. 1 Physical parameters and plane of motion of a two-link manipulator.

For the time-optimal control problem the state is transformed in a minimum time t_f from the initial, $x(0) = x_0$, to the final, $x(t_f) = x_f$, configurations.

The optimal solution must satisfy the following necessary conditions:

$$\dot{x} = \frac{\partial H}{\partial p}, \qquad \dot{p} = -\frac{\partial H}{\partial x} \tag{3}$$

$$H(x, u, p) \xrightarrow{u} \min \tag{4}$$

where the Hamiltonian $H(x, u, p)$ is defined as

$$H(x, u, p) = 1 + p^T[A(x) + C(x)u(t)] \tag{5}$$

and where $p(t)$ is the costate vector.

The control torques, obtained from Eq. (4), have the form of a bang-bang control

$$u_i = \begin{bmatrix} U_i^+ & \text{for} & G_i < 0 \\ U_i^- & \text{for} & G_i > 0 \end{bmatrix} \tag{6}$$

where $G_i = p^T c_i$ is the switch function corresponding to the control u_i, and c_i is the ith column of matrix C. Additionally, the Hamiltonian must satisfy the following target condition:

$$H(x, u, p)_{t_f} = 0 \tag{7}$$

The problem given by the set of differential equations (3), the requirements (6) and (7), and the given initial and final boundary conditions constitutes a TPBVP in which n states and n costates must satisfy $2n$ initial and final boundary conditions imposed on the state only. Here we used the procedure that is essentially based on the shooting method.[1,2] It solves the preceding TPBVP by numerically integrating Eq. (3) with the controls determined from Eq. (6). The switch times of the bang-bang solution are modified iteratively so as to meet the final conditions $x_f = x(t_f)$ and the condition (7) with a predetermined accuracy. For the case presented in the next section the convergence criterion was set to 10^{-6}, which means that the iterations were terminated when the accuracy up to about six significant digits was achieved.

III. Results

The physical parameters of the manipulator are as follows:

$$l_1 = 2l_{c1} = 0.2 \text{ m}, \quad U_1^{\mp} = \mp 10.0 \text{ Nm}, \quad I_1 = 0.004167 \text{ kg} \cdot \text{m}^2$$

$$l_2 = 2l_{c2} = 0.2 \text{ m}, \quad U_2^{\mp} = \mp 5.0 \text{ Nm}, \quad I_2 = 0.004167 \text{ kg} \cdot \text{m}^2$$

$$m_1 = 1.0 \text{ kg}, \qquad m_2 = 1.0 \text{ kg}, \qquad m_a = 0 = m_b$$

A robot with similar parameters was considered in Ref. 6. The effective gravity g varies accordingly with the orientation of the plane of motion from $g = 0$ (horizontal) to $9.81 \text{ m} \cdot \text{s}^{-2}$ (vertical). The rest-to-rest maneuvers from straight-to-straight configurations with the travel angle $\Delta\varphi_1 = 60$ deg are presented here. For comparison, Fig. 2 shows the trajectories of the end of the manipulator for the maneuver in the vertical plane ($\beta = 90$ deg and $g = 9.81$) and in the almost horizontal plane ($\beta = 5.85$ deg and $g = 1.0$). These trajectories look similar, but they have different switching patterns and